[9]  I. Gheorghe, H. J. Rack, *Mater. Sci. Tech.* **2002**, *18*,107.

[10]  A. R. Kennedy, *J. Mater. Sci.* **2002**, *37*, 317.

[11]  D. Ye, J. Hu, *Practical handbook for the thermodynamic data of inorganic substance (2nd edition),* Metallurgy Industry Publishing House, Beijing, **2002**.

# Micron-scale Deformation and Damage Mechanisms of Ti₃SiC₂ Crystals Induced by Indentation**

## By *Zhe-Feng Zhang,* *Zheng-Ming Sun*, *Hui Zhang* and *Hitoshi Hashimoto*

In the past decade, $Ti_3SiC_2$ with different single phase contents have been synthesized by several sintering processes, such as self-propagating high-temperature synthesis (SHS), hot-isotropic-pressure (HIP), solid-liquid sintering.[1–5] Compression, tension and bending tests have been widely applied to $Ti_3SiC_2$ samples at room and elevated temperatures.[3–13] $Ti_3SiC_2$ can display novel mechanical properties through multiple deformation and damage mechanisms, which are relatively complex in comparison with other materials.[4–11,13] However, an open question is that there is a large difference in the fracture strength under compression and tension.[3–11] Therefore, it is worth revealing (1) how many deformation and damage mechanisms can coexist upon loading and (2) how these deformation and damage modes affect the mechanical properties of $Ti_3SiC_2$? Indentation load can induce highly local plasticity in $Ti_3SiC_2$ and therefore is an appropriate method to activate the multiple deformation and damage modes. The hardness tests have been applied to $Ti_3SiC_2$ samples synthesized by SHS, HIP and CVD techniques.[1–5,7,8,14–18]

[*] Prof. Z.-F. Zhang, Dr. H. Zhang
Shenyang National Laboratory for Materials Science
Institute of Metal Research
Chinese Academy of Sciences
Wenhua Road 72, 110016, Shenyang, P. R. China
E-mail: zhfzhang@imr.ac.cn

Dr. Z.-M. Sun, Dr. Hashimoto
National Institute of Advanced Industrial Science and
Technology (AIST Tohoku)
Nigatake 4-2-1, Miyagino-ku, Sendai, 983-8551, Japan

Recently, we developed a low-temperature sintering method, i.e. pulse discharge sintering (PDS), for the synthesis of $Ti_3SiC_2$ materials with high single phase content.[19,20] High-temperature mechanical properties for four-point bending and compression tests showed that the $Ti_3SiC_2$ samples possess relatively good performance.[11,12] In the present work, the deformation and damage mechanisms induced by indentation were investigated for these $Ti_3SiC_2$ samples prepared by the PDS technique in a very wide load range. Most of the indentations were focused to the interior of $Ti_3SiC_2$ grains so that the measured value represents the hardness of single $Ti_3SiC_2$ grains, regardless of the effect of grain boundaries.

*Results and discussion:* Figure 1 shows the dependence of Vickers hardness for the $Ti_3SiC_2$ samples on the applied load. For comparison, some data by Barsoum et al.[8] was also plotted in the figure. When the applied load is smaller than 1 N, all the indentations were performed within one coarse grain, therefore, the measured values represent the hardness of $Ti_3SiC_2$ single crystals. In low load range below 1 N, 20–50 indentations were made for the accuracy of the testing results. In high load range over 10 N, each indentation involves several $Ti_3SiC_2$ grains and 10–20 indentations were made. It can be seen that the average hardness of $Ti_3SiC_2$ crystals decreases with increasing load, and finally reaches a constant value of ~ 4 GPa, which is identical with the previous results.[1–5,7,8,14–18] Nickl et al.[14] by working with small single crystals prepared by CVD, first reported that the anisotropic Knoop hardness normal and parallel to the basal planes are 12-15 GPa and 3-4 GPa, respectively. Pampuch et al.[1] using hot-pressed samples containing some other hard phases, measured a hardness of ~ 6 GPa. Lis et al.[2] measured the hardness of $Ti_3SiC_2$-TiC composites as a function of the TiC content and estimated that the hardness of pure $Ti_3SiC_2$ to be ~ 4 GPa. Barsoum and El-Raghy[3] found that the hardness value of the $Ti_3SiC_2$ samples with single phase content higher than 98 wt% is 4 GPa, which is identical with the estimated value by Lis et al.[2] El-Raghy et al.[7] measured the microhardness of the $Ti_3SiC_2$ samples with different grain sizes (FG $d = 4$ μm; CG $d = 200$ μm). At higher loads ($P = 100$ N), the hardness is ~ 4 GPa, independent of the grain size. The critical indentation load at which the hardness became independent of the indentation load is influenced by the grain size and is typically larger for a larger-grain-sized material.
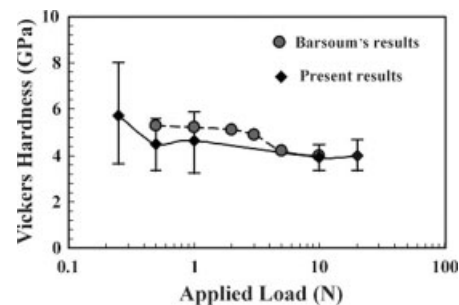


Fig. 1. Dependence of Vickers hardness on the applied load for different $Ti_3SiC_2$ samples.

Recently, Kooi et al.[18] investigated the nano-indentation hardness of Ti$_3$SiC$_2$ with a coarse grained structure in combination with the orientation imaging microscopy (OIM) technique. The surface parallel to the basal plane displayed a low hardness of 4.9 GPa and more plastic deformation than the surface perpendicular to the basal plane. From all the results above, it indicates that the variation of hardness in the lower load range should strongly depend on the orientation of Ti$_3$SiC$_2$ crystals. At the lowest load of 0.25 N, the present hardness ranges of ~ 4–8 GPa, which is identical with the recent results available in other Ti$_3$SiC$_2$ materials.[18] The higher hardness value should correspond to the surface perpendicular to the basal plane, however, the lower hardness value might be associated with the surface parallel to the basal plane. In the higher load range, almost all the reported hardness values are close to ~ 4 GPa, indicating that the grain boundaries play little role in the hardness of the Ti$_3$SiC$_2$ samples.

After deformation by indentation, sliding features were observed to prevail in the Ti$_3$SiC$_2$ grains, as shown in Figure 2a. The sliding has been proved to be along the basal plane, i.e. (0001) plane.[6,13] For all the deformed Ti$_3$SiC$_2$ grains, there is only one group of sliding bands, indicating that only one slip system can be activated under deformation. Normally, the sliding bands are straight and parallel to the basal plane during deformation. However, for the deformed Ti$_3$SiC$_2$ grains, it was frequently observed that the sliding bands can bend to certain degree without the formation of crack, as shown in Figure 2b. The deformation morphology of the Ti$_3$SiC$_2$ grains in Figures 2a and b clearly reveals a ductile feature, which is similar to the slipping in ductile metallic materials. In some local region of the bend bands, crack can form parallel to the basal plane due to separation of the deformation bands, as indicated by an arrow in Figure 2c. This indicates that the shear strain between the bent and unbent layers is incompatible and lead to delamination, which is one of the typical damage modes in Ti$_3$SiC$_2$ crystals.[6,8,11,13,15–18] Another damage mode of Ti$_3$SiC$_2$ is the local cleavage fracture along the plane perpendicular to the shear direction, as indicated by arrows in Figure 2d. The local cleavage fracture can be attributed to the high local tensile stress during severe bending of the deformation bands. From the observations in Figure 2, it is apparent that sliding and buckling are two basic deformation modes for the Ti$_3$SiC$_2$ crystals. There are two damage mechanisms. i.e. delamination and cleavage fracture of the deformation bands, both of which are induced by buckling.

With increasing indentation load, the degree of deformation and damage increases within Ti$_3$SiC$_2$ grains. This in turn leads to a severe buckling and delamination of the deformation bands, as shown in Figures 3a and 3b, which were taken from the samples after indentation under a load of 1 N. The similar deformation and damage mechanisms can be extensively observed in Ti$_3$SiC$_2$ samples subjected to compression and indentation loads.[5–8,11,13,15–18] However, under tensile load, this deformation feature was seldom demonstrated in Ti$_3$SiC$_2$.[5,7–10] Meanwhile, it is noted that the deformation bands can bend to a large angle (Fig. 3b), indicating a good ductility of the Ti$_3$SiC$_2$ crystals. In some Ti$_3$SiC$_2$ grains, another deformation mechanism, i.e. kinking, can be extensively observed, as shown in Figures 3c and 3d. When Ti$_3$SiC$_2$ grain has a suitable orientation, multiple kinking can form with accompanying multiple buckling, delamination and cleavage fracture of deformation bands (see Fig. 3c). Kinking is also a basic deformation mode in Ti$_3$SiC$_2$ samples under compression and indentation.[6,13] Meanwhile, two types of cracks associated with kinking bands can be observed, i.e. delamination and cracking along kinking boundaries (see Fig. 3c). The delamination cracks are triangular in shape with the obtuse angles at the kink boundaries and the acute angles propagating into the materials on both sides of the boundary.[13] The cracks along the kink boundaries are typical cleavage fracture of deformation bands, as shown in Figure 3c. This indicates that both buckling and kinking can cause the damage of grains with the formation of cracks parallel and perpendicular to the deformation bands. However, the easy formation of
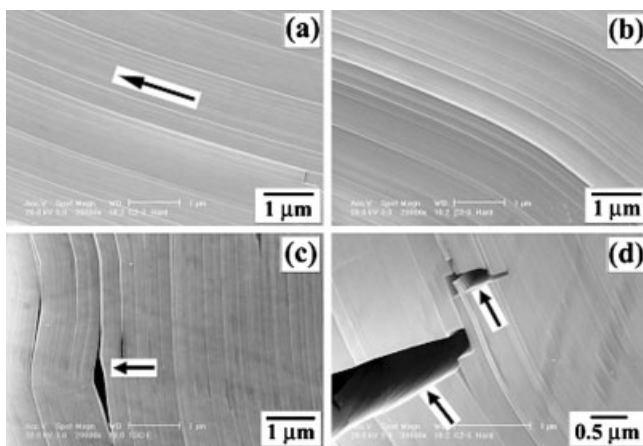


Fig. 2. Typical deformation and damage modes of Ti$_3$SiC$_2$ crystals. (a) Sliding; (b) slight buckling; (c) delamination and (d) local cleavage fracture of the deformation bands. (P = 0.2–0.5 N).
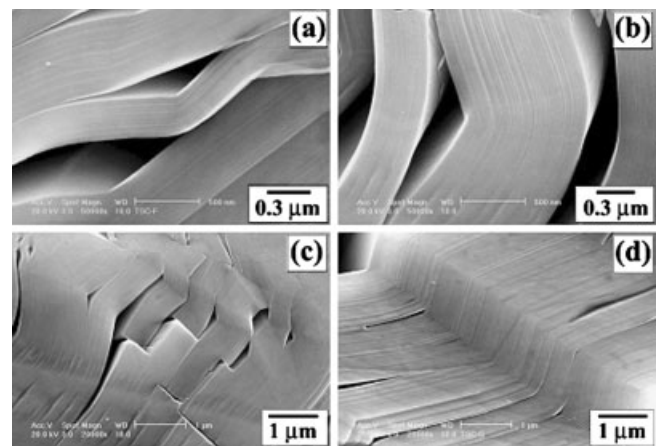


Fig. 3. Typical damage modes of Ti$_3$SiC$_2$ crystals. (a) Cracking along deformation bands; (b) severe buckling and delamination of deformation bands; (c) and (d) kinking. (P = 1 N).

the delamination cracks parallel to the deformation bands induced by buckling and kinking demonstrates a weak bonding of basal plane layers.

With further increasing the indentation load, several $Ti_3SiC_2$ grains took part in the plastic deformation. For all the indentations at different loads (below 20 N), there is complete absence of any cracks near the indentations, which is identical with the previous observations.[8,15–18] El-Raghy et al.[15] investigated the damage mechanisms around hardness indentations in $Ti_3SiC_2$ and found that even at the indentation load of 300 N, no medium or lateral cracks were detected. Therefore, it was considered that $Ti_3SiC_2$ is a damage-tolerant material able to contain the extent of damage in a small area via a number of multiple energy-absorbing mechanisms. Low et al.[16,17] observed the contact damage and deformation near and within the indentation at different stage of loading. They found that the damage is sliding along basal planes and micro-failures along grain boundaries. The grain boundary failure was intersected by the heavily deformed lamellae, analogous to the generation of micro-cracks at dislocation pile-ups in metals and across some of the adjacent grains. The damage consists predominantly of basal-slip lamellae within grains, with accompanying shear-induced micro cracking between grains. SEM observations revealed that crack often extended from the indentation corners on the top surface, but not on the lateral surface. For the present $Ti_3SiC_2$ samples, when the indentation involves several grains, sliding, bending and kinking are abundant within the deformed grains. Except for the damage within $Ti_3SiC_2$ grains, microcracks along grain boundaries become predominately and can be widely observed, as indicated by arrows in Figures 4a and 4b. It seems that grain boundaries are relatively weak and are easy to nucleate intergranular cracks for $Ti_3SiC_2$ polycrystals.

From the observations above, it can be concluded that $Ti_3SiC_2$ displays multiple deformation and damage mechanisms under indentation. Barsoum et al.[13] summarized them as shearing, kinking, buckling and delamination and proposed their formation mechanisms. They considered two $Ti_3SiC_2$ grains with different orientations. When they were subjected to a vertical load, the cavity will form along the grain boundary due to the shearing of one $Ti_3SiC_2$ grain with suitable orientation. This corresponds to the onset of further deformation and damage. The sequence of deformation and damage includes: (1) arrays and shearing deformation; (2) cavitations

and initiation of buckling; (3) kink-band formation; (4) buckling and delamination cracks; (5) damage containment. Barsoum and El-Raghy used orientated polycrystalline $Ti_3SiC_2$ samples with grain size of 1–3 mm. For the present $Ti_3SiC_2$ sample, the grains selected for indentation have a size more than 100 μm, but the indentation size at low indent load is below 20 μm. However, kinking can be widely observed within a single $Ti_3SiC_2$ grain, rather than along grain boundary. This indicates that kinking is a common phenomenon and is easy to form within $Ti_3SiC_2$ grains. Meanwhile, another deformation behavior, i.e. buckling, was also frequently observed after indentation, as shown in Figure 2 and Figure 3. Therefore, there are three fundamental deformation mechanisms for $Ti_3SiC_2$ crystals, i.e. sliding, buckling and kinking, which can form within a single grain. Since there is only one group of slip system in crystals, i.e. $(0001)//[11\bar{2}0]$, sliding can only proceed along (0001) basal plane under a homogeneous shear stress. However, the stress distribution around indentation is often inhomogeneous and the deformation is also complex. One case is that there is relatively homogeneous shear stress subjected to one $Ti_3SiC_2$ grain, meanwhile, another lateral stress also applied to the grain. This will result in buckling of the deformation layers with accompanying the formation of sliding, as shown in Figure 2(b) and Figure 3(b). For the formation of kinking, it can be attributed to a combined effect of the shear stress and two lateral stresses from the opposite directions. In essence, the formation of buckling and kinking can be attributed to two factors: (1) special crystallography, i.e. h.c.p. structure with a high axis ratio of $c/a = 5.8$–$6.0$;[8] (2) complex stress condition. Only one slip system makes it impossible to coordinate the plastic strain of the lateral direction during sliding on the basal plane. Therefore, buckling and kinking become additional deformation modes in $Ti_3SiC_2$ crystals to coordinate the local plastic strain of the lateral direction, however, always leading to the formation of multiple cracks.

According to these clarified deformation and damage mechanisms of the $Ti_3SiC_2$ crystals, a summary map can be established as illustrated in Figure 5. Under deformation, the sliding is the most fundamental deformation mode and always nucleates at first, as shown in Figure 5a. With further deformation, due to inhomogeneous distribution of stress, another two basic deformation modes, i.e buckling and kinking will be activated within the grain, as shown in Figures 5b
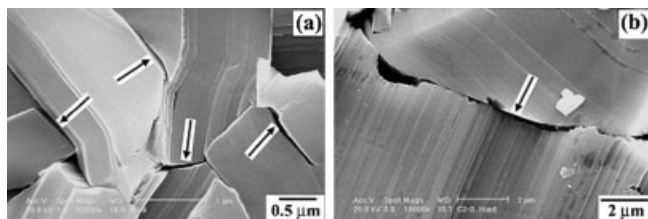


Fig. 4. Intergranular cracking of $Ti_3SiC_2$ polycrystals induced by indentation. (P = 10 N).
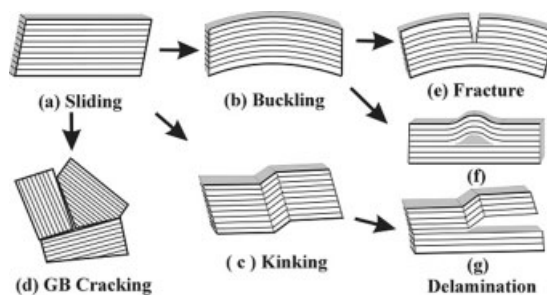


Fig. 5. Deformation and damage map of $Ti_3SiC_2$ crystals induced by indentation.

and 5c. When the sliding propagates to a grain boundary, intergranular cracking is relatively easy to nucleate due to the pile-up of dislocations at the interface, as shown in Figure 5d. Meanwhile, the formation of buckling always accompanies two damage modes, i.e. cleavage fracture and delamination, as illustrated as in Figures 5e and 5f. Also kinking can cause two typical cracks along kinking boundaries and delamination crack, as shown in Figure 5g. Therefore, the plastic strain energy induced by indentation and compression can be absorbed by the multiple deformation and damage mechanisms, including: sliding, buckling, kinking, intergranular and transgraunlar cracking. This often allows a damage-tolerance to long cracks, as in the other brittle ceramic materials.

*Conclusions:* The hardness of $Ti_3SiC_2$ crystals shows load dependence in low load range and reaches a nearly constant value of ~ 4 GPa in the high load range. In the low load range, the orientations of $Ti_3SiC_2$ crystals also affect the hardness, which ranges from 4 to 8 GPa in the present tests.

$Ti_3SiC_2$ crystals have a multiple deformation and damage mechanisms. Sliding, buckling and kinking are three basic deformation mechanisms under indentation. Transgranular and intergranular cracking always lead to the local damage in $Ti_3SiC_2$ polycrystals. Typical transgranular cracking often displays as the formation of delamination crack and cleavage fracture of deformation bands induced by the severe buckling and kinking.

*Experimental*

Commercially available Ti (10 μm and 99.9 %), Si (10 μm and 99.9 %) and TiC (2-5 μm and 99 %) powders with a molar ratio of 1:1:2 were selected in the present experiment. Before sintering, the powder was mixed by a Turbular shaker mixer in Ar atmosphere for 24 h, then, was compacted into a graphite mold (50 mm in diameter) and sintered in vacuum ($10^{-4}$ Torr) at 1400 °C for 60 min by using the PDS technique. The relatively high sintering temperature (1400 °C) as compared to the sintering conditions we usually used for $Ti_3SiC_2$ synthesis can coarsen the $Ti_3SiC_2$ grains.[20] The heating rate was controlled at 50 °C/min and the applied pressure was maintained constant at 50 MPa during sintering. The purity of the sintered $Ti_3SiC_2$ sample was calculated from the x-ray diffraction result to be ~ 95 wt% with the residual TiC phases through standard additive method.[19] Then, the sample was etched by a solution of $H_2O$:$HNO_3$:HF (2:1:1) for 5 – 10 sec to expose the $Ti_3SiC_2$ grains. The microstructure of the $Ti_3SiC_2$ samples consists of 50 – 200 μm lath-like structure and 2–10 μm fine grains. Indentation tests were performed to the etched $Ti_3SiC_2$ samples in a load range of 0.25 – 20 N. After tests, the indentations were observed by SEM to reveal the deformation and damage mechanisms at different loads.

[1] R. Pampuch, J. Lis, J. Piekarczyk, L. Stobierski, *J. Mater. Synth. Proc.* **1993**, *1*, 93.

[2] J. Lis, Y. Miyamoto, R. Pampuch, K. Tanihata, *Mater. Lett.* **1995**, *22*, 163.

[3] M. W. Barsoum, T. El-Raghy, *J. Am. Ceram. Soc.* **1996**, *79*, 1953.

[4] N. F. Gao, Y. Miyamoto, *J. Mater. Sci*, **1999**, *34*, 4385.

[5] J. F. Li, W. Pan, F. Sato, R. Watanabe, *Acta Mater.* **2001**, *49*, 937.

[6] M. W. Barsoum, T. El-Raghy, *Metall. Matall. Trans.* **1998**, *29*, 363.

[7] T. El-Raghy, M. W. Barsoum, A. Zavaliangos, S. R. Kalidindi, *J. Am. Ceram. Soc.* **1999**, *82*, 2855.

[8] M. W. Barsoum, *Prog. Solid State Chem.* **2000**, *28*, 201.

[9] M. Radovic, M. W. Barsoum, T. El-Raghy, J. Seidensticker, S. M. Wiederhorn, *Acta Mater.* **2000**, *48*, 453.

[10] M. Radovic, M. W. Barsoum, T. El-Raghy, S. M. Wiederhorn, W. E. Luecke, *Acta Mater.* **2002**, *50*, 1297.

[11] Z. M. Sun, Z. F. Zhang, H. Hashimoto, T. Abe, *Mater. Trans.* **2002**, *43*, 436.

[12] Z. F. Zhang, Z. M. Sun, H. Hashimoto, *Adv. Eng. Mater,* **2002**, *4*, 864.

[13] M. W. Barsoum, L. Farber, T. El-Raghy, *Metall. Mater. Trans.* **1998**, *29*, 1727.

[14] T. Goto, T. Hirai, *Mater. Res. Bull.* **1987**, *22*, 1195.

[15] T. El-Raghy, A. Zavaliangos, M. W. Barsoum, S. R. Kalidini, *J. Am. Ceram. Soc.* **1997**, *80*, 513.

[16] It M. Low, S. K. Lee, B. R. Lawn, *J. Am. Ceram. Soc.*, **1998**, *81*, 225.

[17] It M. Low, *J. Europ. Ceram. Soc.* **1998**, *18*, 709.

[18] B. J. Kooi, R. J. Poppen, N. J. M. Carvalho, J. Th. M. De Hosson, M. W. Barsoum, *Acta Mater.* **2003**, *51*, 2859.

[19] Z. F. Zhang, Z. M. Sun, H. Hashimoto, *Metall. Mater. Trans.* **2002**, *A33*, 3321.

[20] Z. F. Zhang, Z. M. Sun, H. Hashimoto, T. Abe, *J. Am Ceram. Soc.* **2003**, *86*, 431.

# Structure-Processibility Relationships During Rotational Moulding of Plastics

By *Abbas Tcharkhtchi\** and *Jacques Verdu*

The shape of a plastic part made by rotational moulding (RM) results from coalescence and sintering of granular particles into a liquid state.[1–4] During moulding, the temperature must be sufficiently high to achieve the correct viscous and elastic rheological characteristics in the polymer to promote the coalescence of granular particles, and for the removal of trapped air bubbles. But polymers are characterised by a relatively low thermal stability and their processing temperature cannot be increased indefinitely. The ease with which a successful rotationally moulded plastic part can be produced depends, therefore, on the achievement of an acceptable compromise between two contradictory needs: (a) high tempera-

[*] Prof. A. Tcharkhtchi, Prof. J. Verdu
ENSAM 151 Bd de l'Hôpital
75013 PARIS
E-mail: abbas.tcharkhtchi@paris.ensam.fr